Journal of Power Sources 316 (2016) 224–231

Contents lists available at ScienceDirect

Journal of Power Sources

journal homepage: www.elsevier.com/locate/jpowsour

# Efficient and stable iron based perovskite $La_{0.9}Ca_{0.1}Fe_{0.9}Nb_{0.1}O_{3-\delta}$ anode material for solid oxide fuel cells

Xiaowei Kong [a, c], Xiaoliang Zhou [a, b, **], Yu Tian [a, c, *], Xiaoyan Wu [a, c], Jun Zhang [a, c], Wei Zuo [a, c], Xiaobo Gong [a, c], Zhanhu Guo [d]

[a] State Key Laboratory of Urban Water Resource and Environment, Harbin Institute of Technology (SKLUWRE, HIT), Harbin 150090, PR China
[b] Natural Science Research Center, Academy of Fundamental and Interdisciplinary Sciences, Harbin Institute of Technology, Harbin 150080, PR China
[c] School of Municipal and Environmental Engineering, Harbin Institute of Technology, Harbin 150090, PR China
[d] Integrated Composites Laboratory (ICL), Department of Chemical & Biomolecular Engineering, University of Tennessee, Knoxville, TN 37996, USA

## HIGHLIGHTS

- $La_{0.9}Ca_{0.1}Fe_{0.9}Nb_{0.1}O_{3-\delta}$ (LCFNb) is prepared by Nb doping in $La_{0.9}Ca_{0.1}FeO_{3-\delta}$.
- LCFNb and LCFNb/SDC are stable in both $H_2$ and CO at 850 °C examined by XRD.
- A power density of 823 mW $cm^{-2}$ at 800 °C in $H_2$ is obtained with LCFNb/SDC anode.
- LCFNb/SDC gives a desirable anti-coking ability in CO and syngas for 50 h.
- LCFNb/SDC shows reasonable sulfur tolerance in 100 ppm $H_2S$–$H_2$ for 20 h.

## ARTICLE INFO

*Article history:*
Received 24 January 2016
Received in revised form
20 March 2016
Accepted 21 March 2016
Available online 4 April 2016

*Keywords:*
Solid oxide fuel cell
Perovskite
Wet impregnation
Carbon deposition
Sulfur tolerance

## ABSTRACT

A novel $La_{0.9}Ca_{0.1}Fe_{0.9}Nb_{0.1}O_{3-\delta}$ (LCFNb) perovskite for solid oxide fuel cells (SOFCs) anode is prepared by means of the citrate-nitrate route and composited with $Ce_{0.8}Sm_{0.2}O_{1.9}$ (SDC) by impregnation method to form nano-scaled LCFNb/SDC anode catalytic layers. The single cells with LCFNb and LCFNb/SDC impregnated anodes both achieve relatively high power output with maximum power densities (MPDs) reaching up to 610, 823 mW·$cm^{-2}$ in $H_2$ at 800 °C, respectively, presenting a high potential of LCFNb for use as SOFCs anode. The power outputs of the single cells with LCFNb/SDC composite anode in CO and syngas (CO–$H_2$ mixture) are almost identical to that in $H_2$ at each testing temperature. This composite anode also presents excellent durability in both $H_2$ and CO for as long as 50 h, showing desirable anti-reduction and carbon deposition resistance abilities. Besides, the cell output is stable in 100 ppm $H_2S$–$H_2$ atmospheres for 20 h at a current density of 600 mA·$cm^{-2}$ with negligible sulfur accumulation on the anode surface. Hence, a novel iron based perovskite LCFNb anode with remarkable cell performance, carbon deposition resistance and sulfur poisoning tolerance for SOFCs is successfully obtained.



## 1. Introduction

Solid oxide fuel cell (SOFC) is an environmental friendly and efficient technology to generate electricity from various fuels for energy conversion [1–3]. In order to make commercial applications feasible at low costs, it is necessary to run the SOFC systems with materials inexpensive and easily accessible at intermediate or even lower temperatures [4]. As an important component of the SOFC, anode undertakes the responsibility to catalyze the fuel oxidation and transfer the charges generated from the electrochemical reactions among the triple phase boundaries (TPBs). However, the widely explored Ni-YSZ anode is undermined due to many disadvantages, such as Ni agglomeration in the long run [5], carbon deposition at intermediate temperatures [6,7], as well as catalyst poisoning within sulfur containing fuels [8,9].

* Corresponding author. State Key Laboratory of Urban Water Resource and Environment, Harbin Institute of Technology (SKLUWRE, HIT), Harbin 150090, PR China.
** Corresponding author. State Key Laboratory of Urban Water Resource and Environment, Harbin Institute of Technology (SKLUWRE, HIT), Harbin 150090, PR China.
*E-mail addresses:* xlzhou@hit.edu.cn (X. Zhou), hittianyu@163.com, hit_tianyu@163.com (Y. Tian).

http://dx.doi.org/10.1016/j.jpowsour.2016.03.077
0378-7753/

Thus, alternative anode materiels like copper and ceria compounds, perovskites, pyrochlores and et al. have been reported targeted at dealing with the problems associated with these Ni-based anodes [10,11]. Among them, perovskites with mixed ionic and electronic conduction, such as $PrBaMn_2O_{5+\delta}$ (PBMO) [1], $Pr_{0.4}Sr_{0.6}(Co,Fe)_{0.4}Nb_{0.1}O_{3-\delta}$ (PSCFNb) [2,12], $La_{0.75}Sr_{0.25}Cr_{0.5}Mn_{0.5}O_{3\pm\delta}$ (LSCM) [13,14], La- or Y-doped $SrTiO_3$ (LST/YST) [15–17], $La_{0.7}Sr_{0.3}VO_{3.85}$ (LSV) [18–20], $Sr_2Fe_{2-x}Mo_xO_6$ (SFM) [21], $Sr_2Mg_xMn_{1-x}MoO_{6-\delta}$ (SMMO) [22] and et al., are reported as potential anode materials due to their capacities to greatly enhance the TPB regions [23,24]. Compared with the nickel based anode catalysts, perovskites with a general stoichiometry $ABO_3$ exhibit excellent thermal and mechanical stability in redox atmospheres [25,26], good tolerance to carbon coking [27–31] and resistance to sulfur poisoning [32–34].

Recently, $La_{0.9}Ca_{0.1}FeO_{3-\delta}$ (LCF) perovskite ceramic with low cost has been reported to be an effective and energy-saving oxygen ion transfer membrane for syngas (a mixture of $H_2$ and CO) production from $CH_4$ due to its advantages of high oxygen-ion conductivity and phase stability in both oxidizing and reducing atmospheres [35,36]. However, Fe based perovskites in the anode compartment of a SOFC are reported to be not stable enough due to the very low oxygen partial pressure under the anode operating conditions [37]. Considering that the stability of perovskite could be enhanced by substituting the B-site with a cation having a higher valence [38–40], we used niobium to further stabilize LCF with respect to ensuring the short term stability for SOFCs application. For the novel $La_{0.9}Ca_{0.1}Fe_{0.9}Nb_{0.1}O_{3-\delta}$ (LCFNb) perovskite, $Fe^{3+}$ ions in the B-site can be partially substituted by $Nb^{5+}$ ions due to their similar ionic radiuses (0.0645 nm for $Fe^{3+}$ vs. 0.064 nm for $Nb^{5+}$).

In the present study, $La_{0.9}Ca_{0.1}Fe_{0.9}Nb_{0.1}O_{3-\delta}$ was synthesized by a conventional citrate-nitrate route, following by investigation on the crystallization characteristics and phase stability. Then, electrolyte supported cells with LCFNb/SDC impregnated anode were fabricated and tested within different fuels, like pure hydrogen, carbon monoxide, syngas and sulfur-containing gases at intermediate temperatures in lab scale. The carbon deposition resistance and sulfur tolerance of such cells in CO and $H_2S$–$H_2$ atmospheres were also presented as well as the short term stabilities in such fuels.

## 2. Experimental

### 2.1. Cell fabrication

A conventional citrate-nitrate route was employed to synthesize the precursor solution for impregnation [41–43]. Briefly, stoichiometric amounts of citric acid (CA), $NbC_{10}H_5O_{20}$, $Fe(NO_3)_3\cdot 9H_2O$, $Ca(NO_3)_2\cdot 4H_2O$, $La(NO_3)_3\cdot 6H_2O$, $Sm(NO_3)_3$ and $Ce(NO_3)_3\cdot 6H_2O$ (Analytical grade, all from Aladdin) as the raw materials were subsequently dissolved in deionized water for the synthesis of $La_{0.9}Ca_{0.1}Fe_{0.9}Nb_{0.1}O_{3-\delta}$ and $Ce_{0.8}Sm_{0.2}O_{2-\delta}$ precursor solution, respectively. The complexing ability of citric acid (CA) was used at a ratio of 1.8:1 for CA/total cations in both cases.

The commercial SSZ powder ($Sc_{0.2}Zr_{0.8}O_{2-\delta}$, Tianyao, China) was ball-milled (ND7 Planetary Mill, Nandatianzun, China) thoroughly with ethanol solvent and polyvinyl butyral (PVB) binder for 48 h to prepare the electrolyte slurry, while additional graphite was introduced as pore formers to prepare the anode slurry. The dense electrolyte film and porous anode layer were tape casted and laminated into disks using the as-prepared slurries. The bi-layers were subsequently sintered at 1550 °C for 4 h. The LSM/YSZ (Fuel Cell Materials, USA) cathode layer was then screen printed onto the surface of the electrolyte and then sintered at 1100 °C for 2 h to obtain good binding between the electrode and the electrolyte. The active electrode areas for all cells were 0.16 $cm^2$.

The as-prepared tri-layers were then impregnated with the aqueous solution containing 0.5 M LCFNb or SDC precursor solution in the porous anode side, following with a heat-treating at 450 °C for minutes. The loadings of LCFNb and SDC were measured with an electronic balance and the infiltration procedure was repeated by turns. The final weight increments of LCFNb and SDC were about 40 wt.% and 25 wt.% with respect to the whole weight of the porous anode layer. Finally, the cells with impregnated anode were sintered at 850 °C for 2 h. The obtained anode after infiltration was abbreviated as LCFNb/SDC hereafter for convenience.

### 2.2. Characterization

The as-prepared cells were sealed with ceramic bond (Ceramabond 552, Aremco products, USA) at one end of the ceramic tube. Silver paste (DAD-87, Shanghai Research Institute of Synthetic Resin, China) was used as the current collector for both anode and cathode. A tubular furnace (SK-G08123K, Tianjin Zhonghuan Lab Furnace Co., Ltd, China) was utilized to heat the cells. Before testing, the assembled SOFCs were firstly heated to 700 °C and fed with $H_2$ to ensure proper function. The impregnated cell was electrochemically characterized after the open circuit voltage (OCV) was stabilized for 1 h in $H_2$ at 700 °C. The fuel gas was then switched to CO or $H_2S$–$H_2$ if necessary and the cell was tested again before the temperature was elevated. The anode fuels were fixed at a flow rate of 30 sccm with a mass flow controller (Alicat, USA) and the cathode was exposed to ambient air.

The electrochemical performances were characterized at temperatures ranging from 700 to 800 °C at 50 °C intervals by using an Arbin MSTAT4 electrochemical workstation (Arbin Corporation, USA). The electrochemical impedance spectrum (EIS) was conducted using an AC signal amplitude of 10 mV at open circuit voltage with the impedance frequency ranging from 1 MHz to 0.01 Hz. X-ray diffraction (XRD) patterns were recorded with a conventional X-ray powder diffractometer (PANalytical, operating at 40 kV and 30 mA using CuK$\alpha$ radiation, scanning in the 2$\theta$ range of 10–70° with a 0.5° step and a time collection step of 1 s). The microstructures of the cells before and after testing were observed with a scanning electron microscope (SEM, Hitachi SU8010, Japan) coupled with Oxford energy-dispersive X-ray spectroscopy (EDS, Oxford X-MAX 50 $mm^2$, UK).

## 3. Results and discussion

### 3.1. Phase formation and chemical compatibility

The crystallization of LCFNb powders and chemical compatibility of LCFNb/SDC composite anode needs to be evaluated for technological development of SOFC materials. The LCFNb precursor infiltrated into the porous SSZ matrix was sintered at 850 °C for 2 h to ensure the crystal formation. Investigations on the crystalline structures of the LCFNb powders and LCFNb/SDC/SSZ mixture sintered at 850 °C were conducted by means of XRD technique (Fig. 1). The X-ray characteristic peaks in Fig. 1a indicated that the phase of the LCFNb formed after sintered in air for 2 h matched well with the standard perovskite-type $La_{0.9}Ca_{0.1}FeO_{3-\delta}$ (JCPDS No. 49-1884) with La, Ca sharing the A-site and Fe, Nb sharing the B-site, indicating that the B-site doping of Nb in LCF had no significant influence on the crystalline structure of perovskite. Moreover, the LCFNb crystal showed high reduction stability for it remained the same perovskite structure after reduced in hydrogen for 4 h (Fig. 1b). Compared with the $La_{0.9}Ca_{0.1}FeO_{3-\delta}$ perovskite, which was not stable in hydrogen atmosphere (Fig. S1a), the anti-reduction abilities of the LCFNb in both hydrogen and carbon monoxide atmospheres were

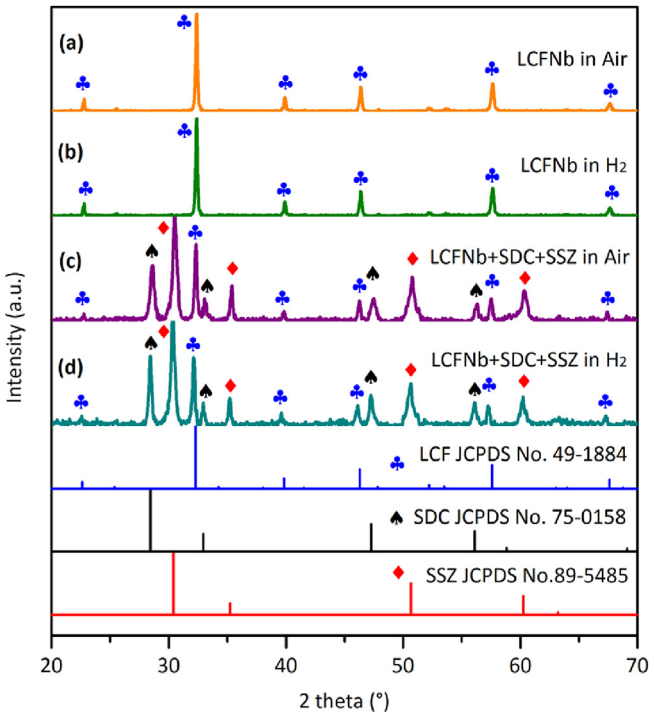


**Fig. 1.** XRD patterns for LCFNb sintered at 850 °C under different conditions: (a) LCFNb crystal sintered in air for 2 h; (b) LCFNb crystal reduced in $H_2$ for 4 h; (c) LCFNb, SDC, SSZ mixture sintered in air for 2 h; (d) LCFNb, SDC, SSZ mixture reduced in $H_2$ for 4 h.

significantly improved owing to the Nb doping in the B-site of the LCF perovskite (Fig. S1c).

To assess the compatibility of LCFNb with SDC and SSZ materials, all the three powders were ball-milled together thoroughly and sintered at 850 °C in both air and hydrogen, and evaluated with the XRD technique as well. The diffraction peaks of the mixtures exhibit a simple mixing of the three phases of LCFNb, SDC and SSZ with no additional diffraction peaks detectable in both air and hydrogen atmospheres, Fig. 1c,d. Thus, there was no clear evidence of reaction for these materials at such a high temperature, which was higher than the temperatures used in the cell testing process, indicating that the LCFNb/SDC/SSZ interfaces were compatible with each other during both the cell preparation and testing operations.

### 3.2. Microstructure analysis and element distribution

The SEM image of cross-sectional porous SSZ anode backbone prior to impregnation was presented in Fig. 2a. The thicknesses of the porous anode and dense electrolyte were about 67 and 58 μm, respectively. The homogeneous, incompact pores with smooth inner surfaces were due to the burn-up of the graphite pore former, among which the crystal of SSZ could be clearly distinguished like tiny hills in Fig. 2b. And, the porosity of the anode layer was estimated to be around 69% by calculating its volume and weight.

When LCFNb and SDC were infiltrated, a deposited layer of LCFNb/SDC was observed as a thin layer covering the inner surface of the backbone (Fig. 2c). As shown in Fig. 2d, the LCFNb/SDC layer (~200 nm) not only appeared to be compatible with each other with no obvious delamination, but also had a solid connection with the SSZ electrolyte. Small pores in the connected network of the LCFNb/SDC layer were also observed in the inset of Fig. 2d, which was beneficial for the transfer and diffusion of the fuel gas in and out of the anode. As a result, the deposited layer with numerous micropores could effectively expand the reaction zone beyond the TPBs.

### 3.3. Electrochemical performance

To primarily evaluate the potential of LCFNb serving as anode component, the cells with LCFNb single impregnated anode and LCFNb/SDC impregnated composite anode were electrochemically characterized. Here, the SDC was used as additional ion transfer channels to expand the reaction zone in the TPBs [44–46]. The voltage and power density as a function of current density for the cells with hydrogen as a fuel and ambient air as an oxidant is shown in Fig. 3. The open-circuit voltages of the cells with different anodes were all around 1.10 V at all the tested temperatures, which were close to the expected Nernst potentials [47], indicating that the SSZ electrolyte films were crack-free and gas-tight with no gas leakage through the electrolyte and ceramic sealant. The cell with LCFNb single impregnated anode exhibited maximum power densities (MPDs) of 370, 521 and 610 $mW \cdot cm^{-2}$ in pure $H_2$ at 700, 750, and 800 °C, respectively, indicating that the LCFNb perovskite has good catalytic activity for anode fuels at all tested temperatures. The MPDs of 395, 590 and 823 $mW \cdot cm^{-2}$ were achieved for the cell with LCFNb/SDC impregnated composite anode at 700, 750, and 800 °C, respectively, which were 7%, 17%, 32% much higher than that of the cell with LCFNb single impregnated anode, owing to the additional infiltration of the SDC. Although the performance of the cell with and without SDC is almost same at the temperature of 700 °C, it is found that the SDC addition greatly enhanced the cell performance at relatively high temperatures. However, it is worth noting that the cell performance is acceptable if there is no SDC addition at all tested temperatures, indicating the LCFNb anode has good electrochemical performance.

According to the literature [48,49], ceria based electrolytes such as SDC and GDC are considered to be the most promising electrolyte materials for IT-SOFC owing to the high ionic conductivity especially at low temperatures. Hence, in the LCFNb/SDC composite anode, the SDC here ought to mainly function as the oxygen ion channel in company with the SSZ. While, the LCFNb with mixed ionic electronic conductivity should be the primary phase for electronic conduction and the main electrocatalyst for direct oxidations of fuels like $H_2$. Thus, in comparison with the LCFNb single impregnated anode, the SDC infiltrated into the composite anode enhanced the oxygen ion conductivity of the anode and expanded the reaction zone in the active TPBs along with the phase interfaces of the LCFNb and SSZ particles. On the other hand, doped ceria materials were proved to have some amounts of electronic conductivity when exposed to the anode reducing atmosphere due to the reduction of $Ce^{4+}$ to $Ce^{3+}$ [50,51]. Consequently, the electronic conductivity of the anode was also enhanced and the electrochemical catalytic activity was further improved owing to the oxygen ion storage & release as well as the transfer capacity of the variable valence cerium ions. Briefly, SDC here is used as the additional oxygen ion transfer channels and fuel catalyst due to its variable valence cerium ions, which is demonstrated to greatly expand the active reaction zone in the TPBs and enhance the catalytic activity.

Here, it was remarkable that the present cells exhibited competitive performance compared with those of recently fabricated electrolyte supported SOFCs (ES-SOFC) with $ABO_3$-doped $CeO_2$ composite anode. For example, the cell fabricated with $SrTi_{0.3}Fe_{0.7}O_{3-\delta}$ (STF)/$Ce_{0.8}Gd_{0.2}O_{2-\delta}$ (GDC) composite anode, $La_{0.9}Sr_{0.1}Ga_{0.8}Mg_{0.2}O_{3-\delta}$ (LSGM) electrolyte and $La_{0.6}Sr_{0.4}Fe_{0.8}Co_{0.2}O_{3-\delta}$ (LSFC) cathode, only showed a MPD of 337 $mW \cdot cm^{-2}$ at 800 °C fed with humidified hydrogen [52]. Besides, the obtained high power output in our study was also more inspiring than what have been reported by C.D. Savaniu [53] and K.B. Yoo [54] et al., by whom the cells with $ABO_3$-doped $CeO_2$ impregnated composite anode were additionally infiltrated by metal catalysts like Ni and

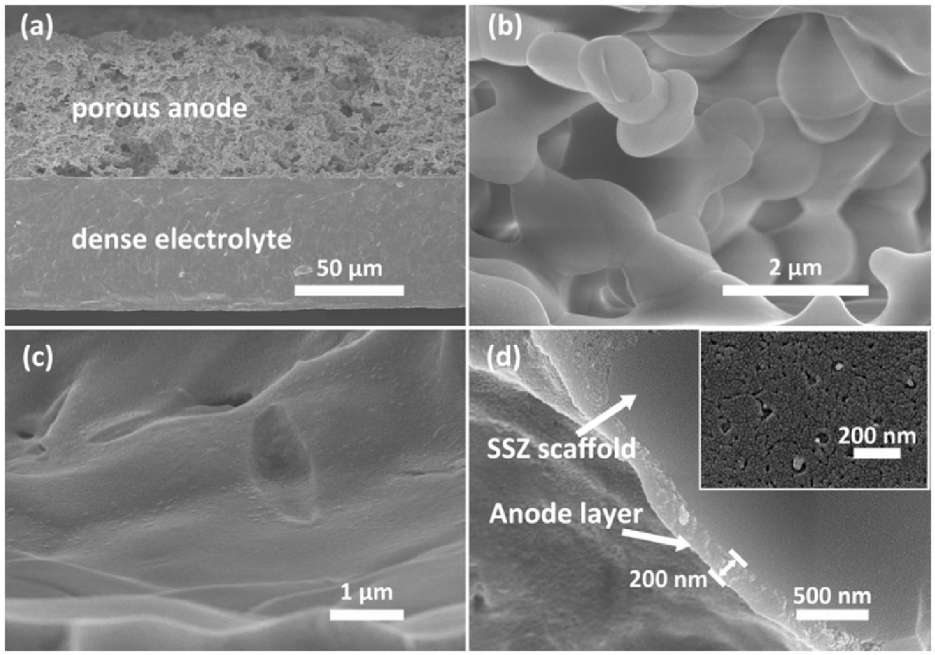


**Fig. 2.** SEM images of: (a) the cross section of SSZ porous anode and dense electrolyte backbone without cathode; (b) the magnified detail of porous anode cross section; (c) the anode surface after LCFNb/SDC impregnation; (d) the cross-sectional view of the LCFNb/SDC infiltrated layer, and the inset of (d) shows the surface detail of the LCFNb/SDC layer.

Cu. And what's more important is that more improvements in the LCFNb based anode may be expected if the electrode structures and cell fabrication processes are further optimized.

### 3.4. Electrochemical impedance spectra

The electrochemical impedance spectra of the cells with impregnated anode under open-circuit conditions are illustrated in Fig. 4. As is known to all, the total resistance of an SOFC can be divided into ohmic resistance ($R_\Omega$) and electrode polarization resistance ($Rp$). Specifically, the ohmic resistances of the two cells, which mainly included the electrolyte resistance of oxygen-ion conduction, electrode ohmic resistance and interface contact resistance, were both about 0.14, 0.13, 0.12 $\Omega\cdot cm^2$ at 700, 750 and 800 °C. The decline of the $R_\Omega$ with the temperature increment was due to the temperature dependence of the ion conductivity. For the cell with LCFNb single impregnated anode, the electrode polarization loss was higher than that of the cell with LCFNb/SDC composite anode at all the tested temperatures. In detail, the polarization resistances of 0.35, 0.50, 0.82 $\Omega\cdot cm^2$ were obtained for the LCFNb single infiltrated cell at 700, 750 and 800 °C, higher than those of 0.34, 0.45, 0.61 $\Omega\cdot cm^2$ for the cell with composite LCFNb/SDC anode, respectively. Comparing with the cell without the SDC, the dramatic decrease of the electrode polarization resistance ($Rp$), which mainly included electrode activation polarization and concentration polarization, suggested that the infiltrated SDC had a significant influence on reducing the electrode polarization losses [16].

As continuous network of LCFNb/SDC conducting channel was gradually formed along with the sequential impregnation, the added LCFNb and SDC particles would gradually fill up the pores in anode and reduce the porosity of the SSZ anode framework, bringing about more limitation on the gas diffusion. However, the I–V relationship was nearly linear even at high current density, which means that the gas transfer process did not become the rate-determining step (RDS) and the electrodes were sufficiently porous to avoid concentration polarization even at high temperatures and large polarization current density conditions. This was also bolstered by the high porosity and porous surface in the impregnated anode as shown in the SEM picture from Fig. 2d, where the thickness of the impregnated layer was only about 200 nm and the micron and sub-micron pores were maintained after infiltration.

### 3.5. Carbon resistance and sulfur tolerance

Cells with LCFNb/SDC composite anode also have shown superior power density and stability in syngas (CO: $H_2$ = 1:1 in volume) and pure CO atmospheres. The MPDs of the cells tested here achieved 409, 577 and 798 $mW\cdot cm^{-2}$ in syngas (Fig. 5), and 380, 541 and 742 $mW\cdot cm^{-2}$ in pure CO (Fig. S2a) at 700, 750 and 800 °C, respectively, which were very close to the MPDs tested in pure $H_2$. The EIS data of the cell with composite anode exhibited just the same polarization resistance in the CO atmosphere as the same cell did in the $H_2$, indicating that the catalytic activities of LCFNb anode in CO and $H_2$ were approximately equivalent (Fig. S2b). Thus, compared with the state-of-the-art Ni-YSZ anode, the LCFNb/SDC composite anode shows a potential way to lower the operating temperature of SOFC below 800 °C with high performance but no carbon deposition. Additionally, as the operating temperature is reduced, much cheaper materials like ferrite here may be employed to not only improve the reliability and operational life of fuel cells but also considerably reduce the costs, making them more commercially viable. The demonstrated coking tolerance and high performance of LCFNb/SDC anode in CO or syngas at lower temperatures therefore advances the possibility for efficient conversion of other hydrocarbon fuels to electricity.

Considering that sulfur species such as $H_2S$ are widely present as main impurity in many hydrocarbon fuels like coal syngas, the sulfur tolerance of SOFC anode becomes an important factor influencing the commercialization of SOFC. Here, the sulfur tolerance of the LCFNb/SDC composite anode was examined under pure $H_2$ and 100 ppm $H_2S$–$H_2$ atmospheres for comparison, and the cell performances were presented in Fig. 6. Initially, the impregnated cell exhibited an OCV of around 1.10 V and a MPD of about

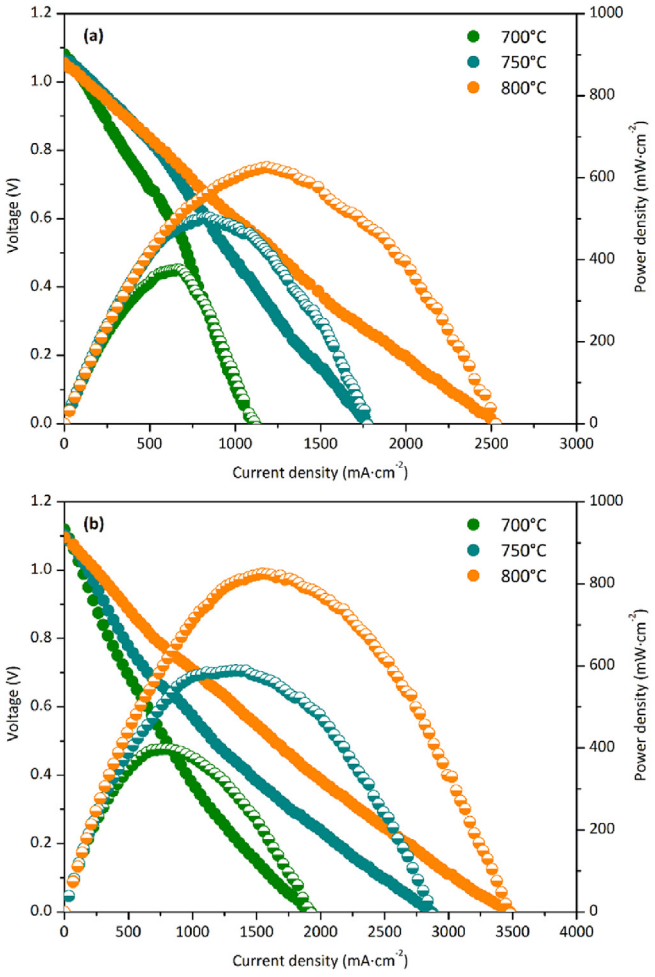


**Fig. 3.** I–V curves of the as-prepared SOFCs in pure $H_2$ with: (a) LCFNb single anode; (b) LCFNb/SDC composite anode.

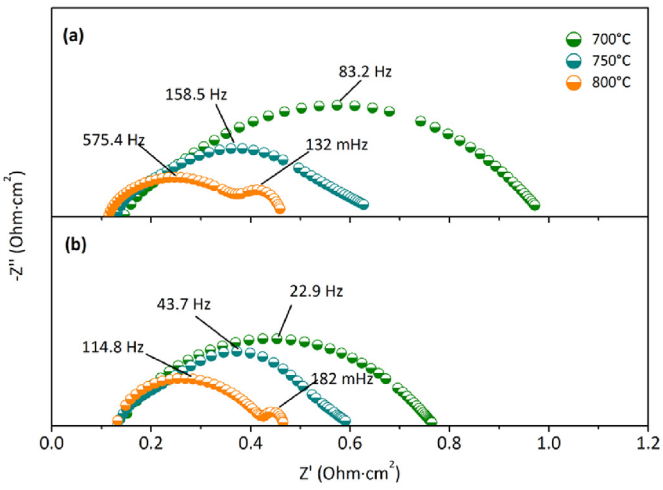


**Fig. 4.** The electrochemical impedance spectra of the as-prepared SOFCs in $H_2$ with: (a) LCFNb single anode and (b) LCFNb/SDC composite anode.

401 mW·cm$^{-2}$ at 700 °C in hydrogen, shown in Fig. 6a, which had a good consistency with the cell with the composite anode tested in hydrogen previously in this paper. When the fuel was switched to 100 ppm $H_2S$–$H_2$ at 700 °C, the cell showed clearly a drop of MPD

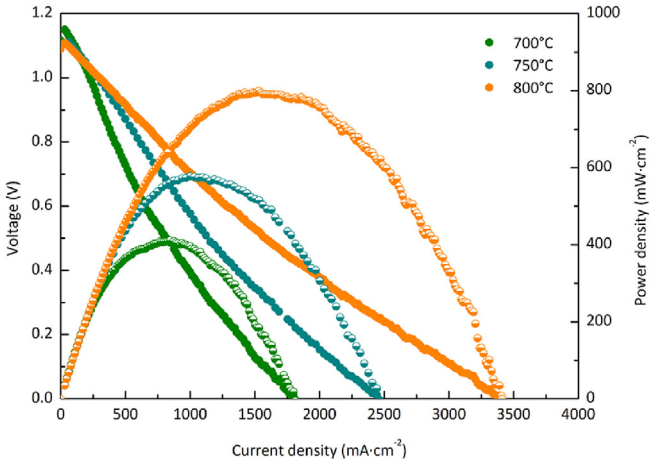


**Fig. 5.** I–V and I–P curves of the as-prepared SOFC with LCFNb/SDC composite anode in syngas.

to 376 mW·cm$^{-2}$. Here, the sulfur-containing fuels did have an adverse effect on the cell performance, but such high $H_2S$ concentration did not result in the failure of the whole cell system. As indicated in Fig. 6b, the electrode polarization rather than the ohmic loss increased clearly with the appearance of $H_2S$. One reasonable explanation was that a small part of the active sites along the TPBs might be blocked due to the interaction of sulfur with anode materials, which had a direct influence on the activation polarization.

With the increment of the testing temperatures, the power output increased and the polarization loss decreased as shown in Fig. 6, which exhibited the same trends as what have been discussed in this paper when the cell was fed with $H_2$ as an anode fuel. Another impregnated cell prepared with the same process was also fabricated and tested in 50 ppm $H_2S$–$H_2$ (Fig. S3), which verified that the experimental results was reproducible.

### 3.6. Short term stability of the cell in various fuels

In order to realize commercially viable intermediate temperature-SOFCs, the durability of constituent materials is one of the most important factors. Here, to further study the stability of the LCFNb/SDC composite anode in different fuels, short term tests for the cells fueled with $H_2$, CO, 50 ppm $H_2S$–$H_2$, 100 ppm $H_2S$–$H_2$ were performed at 750 °C, respectively. The current densities were fixed at 400 mA·cm$^{-2}$ for the cells fed with hydrogen and carbon monoxide, and 600 mA·cm$^{-2}$ for the cells fueled with sulfur containing hydrogen. The initial output voltages were among 0.8–0.9 V for the four cells, as shown in Fig. 7.

The LCFNb/SDC composite anodes seemed to have a reasonable stability and durability during the 50 h tests in $H_2$, CO and syngas (Fig. 7a). It suggested again that the LCFNb/SDC composite anode was not decomposing within the reducing atmosphere like hydrogen (Fig. 1b) and carbon monoxide (Fig. S2c). It also further confirmed that the carbon resistance of the novel LCFNb/SDC composite anode was favorable for the hydrocarbon fuels.

With regard to the sulfur tolerance, cells fed with different $H_2S$ concentration also exhibited negligible degradation in the 20 h test (Fig. 7b), indicating that LCFNb/SDC was electrochemically stable under these conditions. Although we found the power outputs of LCFNb/SDC anodes decreased with the addition of $H_2S$ in the I–V curves from Fig. 6c at 750 °C, here it seemed that the LCFNb/SDC composite anode was not suffering from sulfur poisoning problems

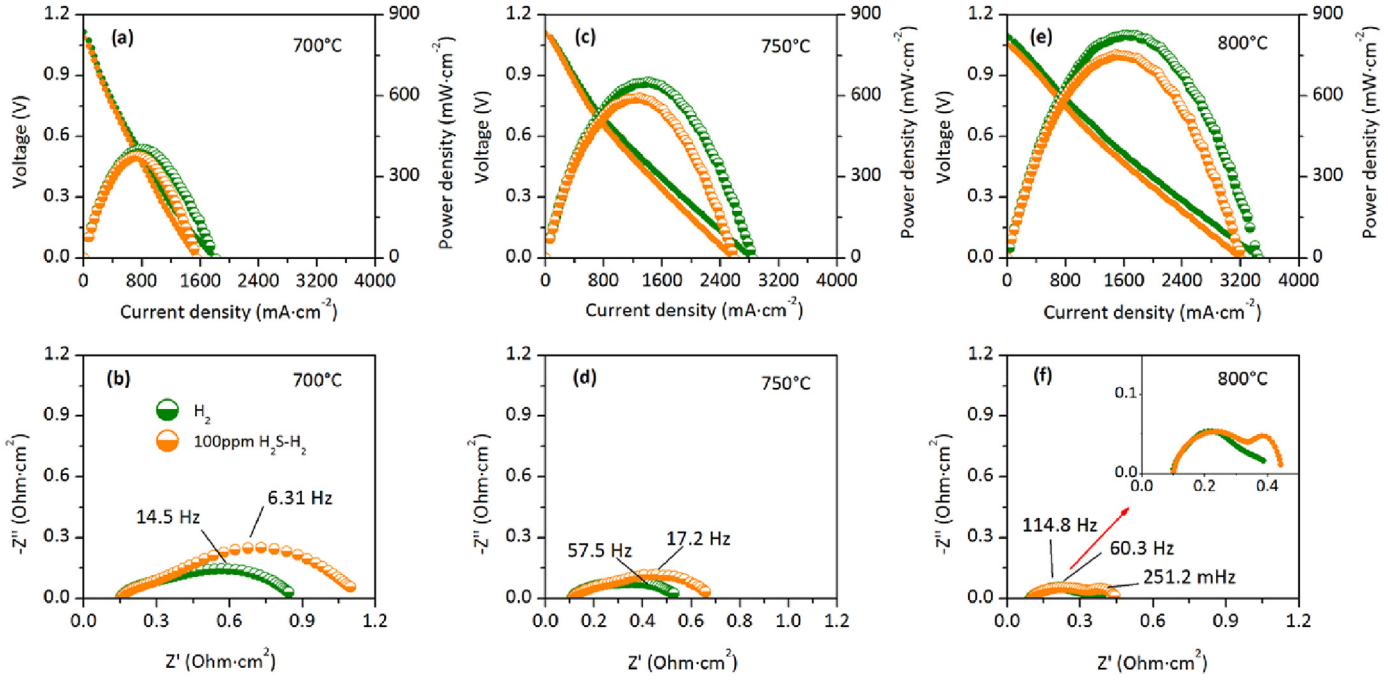


**Fig. 6.** I–V and I–P curves and electrochemical impedance spectra of the as-prepared SOFCs with LCFNb/SDC impregnated anode in $H_2$ (olive symbols) and 100 ppm $H_2S$–$H_2$ (orange symbols): (a,b) 700 °C; (c,d) 750 °C and (e,f) 800 °C. (For interpretation of the references to colour in this figure legend, the reader is referred to the web version of this article.)

associated with the Ni cermets in $H_2S$-containing fuels in the long run [5].

The SEM microstructures of the cells after short term stability tests in all the fuels showed no obvious change of the anode structure but a small amount of insignificant morphological changes in the anode surface, which can be seen from the SEM images shown in Fig. S4. The EDS spectra of the same samples showed that no detectable carbon or sulfur was deposited on the surface of the anode during the short term stability tests (Fig. S5). As a matter of fact, the morphological changes were also observed on the anode surface after the long term stability tests in both hydrogen and carbon monoxide in our study and also have been

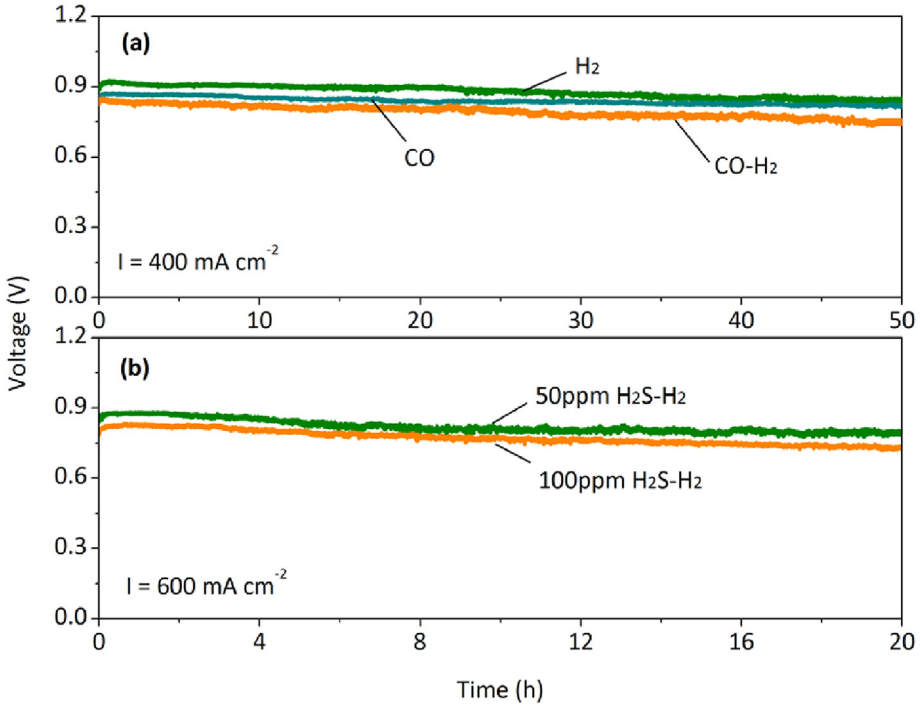


**Fig. 7.** The short term stability tests at 750 °C with the current density be fixed at: (a) 400 mA·cm$^{-2}$ for the three cells in $H_2$, CO and syngas; and (b) 600 mA·cm$^{-2}$ for the two cells in $H_2S$–$H_2$.

found for other perovskites for instance LCF [35,55] and $La_{0.8}Sr_{0.2}Cr_{0.5}Mn_{0.5}O_{3-\delta}$ [56]. As noted earlier, XRD results indicated that the LCFNb remains a single phase perovskite after reduction either in hydrogen or in carbon monoxide, reasonably ruling out the chemical change in the anode materials. A. S. Yu et al. [35] reported the similar findings when they studied the oxygen permeation membrane of LCF, and they attributed this to the changes in the surface free energy under the reducing atmospheres. X. Y. Wu et al. [55] found the grains became coarse on the sweep side when they studied hydrogen generation from water using the LCF oxygen permeation membranes. Through comparing the XRD patterns of the new and the used membrane surfaces, the sweep side shows very LCF-91 peaks despite the changes on the morphologies. While from another perspective, the surface area resulted from the morphological change could be increased and provide more reaction sites for anode electrochemical processes.

As the cell performance didn't keep declining during the short term tests in $H_2S$–$H_2$, a saturation adsorption capacity of sulfur on the anode surface or else might be responsible for the results obtained if any, which was hypothesized that the reduction of sulfur adsorption on oxide anode materials contributed to the enhanced sulfur tolerance in the long run, according to the literature reviewed by Z. Cheng et al. [57].

## 4. Conclusions

In this paper, a novel iron based $La_{0.9}Ca_{0.1}Fe_{0.9}Nb_{0.1}O_{3-\delta}$ (LCFNb) perovskite has been synthesized through partially replacing Fe with Nb in the B site and demonstrated as a potential SOFC anode material with high electrochemical performance, structure stability, carbon resistance and sulfur tolerance in $H_2$, CO and $H_2S$–$H_2$ atmospheres. The electrolyte supported SOFC with LCFNb/SDC impregnated composite anode, SSZ electrolyte and LSM cathode achieved a relatively high maximum power density of 823 $mW \cdot cm^{-2}$ in $H_2$ at 800 °C, showing a high potential of LCFNb for being used as an SOFC anode. The LCFNb/SDC composite anode also exhibited very similar power output in carbon monoxide to that in hydrogen at all the tested temperatures, indicating a good carbon resistance of such materials. Additionally, the cell demonstrated good stability within hydrogen and carbon monoxide atmospheres for 50 h as well as high sulfur tolerance in 100 ppm $H_2S$–$H_2$ during a 20 h testing. The results indicate this novel economical ceramic anode presents high potential application for SOFCs.

## Acknowledgements

This study was supported by the Major Science and Technology Program for Water Pollution Control and Management (No. 2013ZX07201007), the State Key Laboratory of Urban Water Resource and Environment, Harbin Institute of Technology (No. 2014DX03) and the Specialized Research Fund for the Doctoral Program of Higher Education (No. 20112302110060). The authors also appreciate the Heilongjiang Science and Technology Innovation Platform Program for Equipment manufacturing (ZB201307201) and the Science Fund for Distinguished Young Scholars of Heilongjiang Province (JC201303). The authors also thanks funding from the Heilongjiang Postdoctoral Science Foundation (LBH-Z14093) and Fundamental Research Funds for the Central Universities (HIT. NSRIF. 2015096).

## Appendix A. Supplementary data

Supplementary data related to this article can be found at http://dx.doi.org/10.1016/j.jpowsour.2016.03.077.

## References

[1] S. Sengodan, S. Choi, A. Jun, T.H. Shin, Y.W. Ju, H.Y. Jeong, J. Shin, J.T. Irvine, G. Kim, Nat. Mater. 14 (2014) 205–209.
[2] C. Yang, Z. Yang, C. Jin, G. Xiao, F. Chen, M. Han, Adv. Mater. 24 (2012) 1439–1443.
[3] Z. Shao, S.M. Haile, Nature 431 (2004) 170–173.
[4] E.D. Wachsman, K.T. Lee, Science 334 (2011) 935–939.
[5] S.P. Jiang, J. Mater. Sci. 38 (2003) 3775–3782.
[6] C. Sun, U. Stimming, J. Power Sources 171 (2007) 247–260.
[7] J.B. Goodenough, Y.H. Huang, J. Power Sources 173 (2007) 1–10.
[8] M. Błesznowski, J. Jewulski, A. Zieleniak, Open Chem. 11 (2013) 960–967.
[9] K. Sasaki, K. Haga, T. Yoshizumi, D. Minematsu, E. Yuki, R. Liu, C. Uryu, T. Oshima, T. Ogura, Y. Shiratori, J. Power Sources 196 (2011) 9130–9140.
[10] S.P. Shaikh, A. Muchtar, M.R. Somalu, Renew. Sustain. Energy Rev. 51 (2015) 1–8.
[11] N. Mahato, A. Banerjee, A. Gupta, S. Omar, K. Balani, Prog. Mater. Sci. 72 (2015) 141–337.
[12] G. Xiao, S. Wang, Y. Lin, Y. Zhang, K. An, F. Chen, ACS Appl. Mater. Interfaces 6 (2014) 19990–19996.
[13] T. Wenyi, Z. Qin, Y. Han, Z. Xiufang, L. Hongyi, Int. J. Hydrogen Energy 37 (2012) 7398–7404.
[14] X. Zhu, Z. Lü, B. Wei, K. Chen, M. Liu, X. Huang, W. Su, J. Power Sources 195 (2010) 1793–1798.
[15] V. Yurkiv, G. Constantin, A. Hornes, A. Gondolini, E. Mercadelli, A. Sanson, L. Dessemond, R. Costa, J. Power Sources 287 (2015) 58–67.
[16] X. Zhou, N. Yan, K.T. Chuang, J. Luo, RSC Adv. 4 (2014) 118–131.
[17] P. Puengjinda, H. Muroyama, T. Matsui, K. Eguchi, J. Power Sources 216 (2012) 409–416.
[18] C. Ni, J. Vohs, R. Gorte, J. Irvine, J. Mater. Chem. A 2 (2014) 19150–19155.
[19] J.S. Park, J. Luo, L. Adijanto, J. Vohs, R. Gorte, J. Power Sources 222 (2013) 123–128.
[20] J.S. Park, I.D. Hasson, M.D. Gross, C. Chen, J. Vohs, R. Gorte, J. Power Sources 196 (2011) 7488–7494.
[21] G. Xiao, Q. Liu, X. Dong, K. Huang, F. Chen, J. Power Sources 195 (2010) 8071–8074.
[22] Y.H. Huang, R.I. Dass, Z.L. Xing, J.B. Goodenough, Science 312 (2006) 254–257.
[23] Z. Cao, Y. Zhang, J. Miao, Z. Wang, Z. Lü, Y. Sui, X. Huang, W. Jiang, Int. J. Hydrogen Energy 40 (2015) 16572–16577.
[24] X. Zhu, Z. Lü, B. Wei, X. Huang, Y. Zhang, W. Su, J. Power Sources 196 (2011) 729–733.
[25] Y. Zhao, C. Xia, L. Jia, Z. Wang, H. Li, J. Yu, Y. Li, Int. J. Hydrogen Energy 38 (2013) 16498–16517.
[26] N. Lakshminarayanan, J.N. Kuhn, S.A. Rykov, J.-M.M. Millet, U.S. Ozkan, Catal. Today 157 (2010) 446–450.
[27] H. Li, Y. Tian, Z. Wang, F. Qie, Y. Li, RSC Adv. 2 (2012) 3857–3863.
[28] Y.H. Huang, G. Liang, M. Croft, M. Lehtimaki, M. Karppinen, J.B. Goodenough, Chem. Mater. 21 (2009) 2319–2326.
[29] X. Zhu, Z. Lü, B. Wei, K. Chen, M. Liu, X. Huang, W. Su, J. Power Sources 190 (2009) 326–330.
[30] J. Wan, J. Zhu, J. Goodenough, Solid State Ion. 177 (2006) 1211–1217.
[31] S. McIntosh, R.J. Gorte, Chem. Rev. 104 (2004) 4845–4866.
[32] A.L. Vincent, J.L. Luo, K.T. Chuang, A.R. Sanger, Appl. Catal. B Environ. 106 (2011) 114–122.
[33] L. Yang, S. Wang, K. Blinn, M. Liu, Z. Liu, Z. Cheng, M. Liu, Science 326 (2009) 126–129.
[34] R. Mukundan, E.L. Brosha, F.H. Garzon, Electrochem. Solid-State Lett. 7 (2004) A5–A7.
[35] A.S. Yu, J. Kim, T.S. Oh, G. Kim, R.J. Gorte, J.M. Vohs, Appl. Catal. A General 486 (2014) 259–265.
[36] T.C. Geary, S.B. Adler, Solid State Ion. 253 (2013) 88–93.
[37] B.A. Boukamp, Nat. Mater. 2 (2003) 294–296.
[38] T. Nagai, W. Ito, T. Sakon, Solid State Ion. 177 (2007) 3433–3444.
[39] Y. Cheng, H. Zhao, D. Teng, F. Li, X. Lu, W. Ding, J. Membr. Sci. 322 (2008) 484–490.
[40] F. Wang, T. Nakamura, K. Yashiro, J. Mizusaki, K. Amezawa, Solid State Ion. 262 (2014) 719–723.
[41] A.O. Turky, M.M. Rashad, M. Bechelany, Mater. Des. 90 (2016) 54–59.
[42] M. Idrees, M. Nadeem, S.A. Siddiqi, R. Ahmad, A. Hussnain, M. Mehmood, Mater. Chem. Phys. 162 (2015) 652–658.
[43] M.O. Mazan, A.F. Craievich, E.B. Halac, M.C.A. Fantini, D.G. Lamas, S.A. Larrondo, Ceram. Int. 41 (2015) 13721–13730.
[44] Z. Liu, B. Liu, D. Ding, M. Liu, F. Chen, C. Xia, J. Power Sources 237 (2013) 243–259.
[45] L. Zhang, Y. Liu, Y. Zhang, G. Xiao, F. Chen, C. Xia, Electrochem. Commun. 13 (2011) 711–713.
[46] X. Zhu, Z. Lü, B. Wei, K. Chen, M. Liu, X. Huang, W. Su, Electrochem. Solid-State Lett. 12 (2009) B161–B164.
[47] T. Kudo, H. Obayashi, J. Electrochem. Soc. 123 (1976) 415–419.
[48] N. Mahato, A. Gupta, K. Balani, Nanomater. Energy 1 (2012) 27–45.
[49] P. Arunkumar, M. Meena, K.S. Babu, Nanomater. Energy 1 (2012) 288–305.
[50] C. Milliken, S. Guruswamy, A. Khandkar, J. Electrochem. Soc. 146 (1999) 872–882.
[51] A. Atkinson, Solid State Ion. 95 (1997) 249–258.

[52] S. Cho, D.E. Fowler, E.C. Miller, J.S. Cronin, K.R. Poeppelmeier, S.A. Barnett, Energy Environ. Sci. 6 (2013) 1850–1857.
[53] C.D. Savaniu, D.N. Miller, J.T. Irvine, J. Am. Ceram. Soc. 96 (2013) 1718–1723.
[54] K.B. Yoo, G.M. Choi, Solid State Ion. 192 (2011) 515–518.
[55] X.Y. Wu, L. Chang, M. Uddi, P. Kirchen, A.F. Ghoniem, Phys. Chem. Chem. Phys. 17 (2015) 10093–10107.
[56] G. Kim, S. Lee, J. Shin, G. Corre, J. Irvine, J. Vohs, R.J. Gorte, Electrochem. Solid-State Lett. 12 (2009) B48–B52.
[57] Z. Cheng, J.H. Wang, Y. Choi, L. Yang, M. Lin, M. Liu, Energy Environ. Sci. 4 (2011) 4380–4409.